HHS Public Access

Author manuscript

J Am Chem Soc. Author manuscript; available in PMC 2015 August 14.

Published in final edited form as:

J Am Chem Soc. 2013 December 26; 135(51): 19064–19067. doi:10.1021/ja409896y.

Spectral Tuning of Ultraviolet Cone Pigments: An Interhelical Lock Mechanism

Sivakumar Sekharan[†,*], **Victoria L. Mooney**[†], **Ivan Rivalta**[†], **Manija A. Kazmi**[‡], **Maureen Neitz**[§], **Jay Neitz**[§], **Thomas P. Sakmar**[‡], **Elsa C. Y. Yan**[†,*], and **Victor S. Batista**[†,*]

[†]Department of Chemistry, Yale University, New Haven, Connecticut 06520-8107United States

[‡]Laboratory of Chemical Biology and Signal Transduction, Rockefeller University, New York, New York 10065, United States

[§]School of Medicine, Department of Ophthalmology, University of Washington, Seattle, Washington 98195, United States

Abstract

Ultraviolet (UV) cone pigments can provide insights into the molecular evolution of vertebrate vision since they are nearer to ancestral pigments than the dim-light rod photoreceptor rhodopsin. While visible-absorbing pigments contain an 11-*cis* retinyl chromophore with a protonated Schiff-base (PSB11), UV pigments uniquely contain an unprotonated Schiff-base (USB11). Upon F86Y mutation in model UV pigments, both the USB11 and PSB11 forms of the chromophore are found to coexist at physiological pH. The origin of this intriguing equilibrium remains to be understood at the molecular level. Here, we address this phenomenon and the role of the USB11 environment in spectral tuning by combining mutagenesis studies with spectroscopic (UV–vis) and theoretical [DFT-QM/MM (SORCI+Q//B3LYP/6-31G(d): Amber96)] analysis. We compare structural models of the wild-type (WT), F86Y, S90A and S90C mutants of Siberian hamster ultraviolet (SHUV) cone pigment to explore structural rearrangements that stabilize USB11 over PSB11. We find that the PSB11 forms upon F86Y mutation and is stabilized by an “inter-helical lock” (IHL) established by hydrogen-bonding networks between transmembrane (TM) helices TM6, TM2, and TM3 (including water w2c and amino acid residues Y265, F86Y, G117, S118, A114, and E113). The findings implicate the involvement of the IHL in constraining the displacement of TM6, an essential component of the activation of rhodopsin, in the spectral tuning of UV pigments.

During the molecular evolution of vertebrate vision, the ultraviolet (UV) cone pigment acquired structural and functional features that are transitional between those of long-wavelength cone and rhodopsin rod photoreceptors. Five classes of visual pigments have evolved (Figure 1A), including rhodopsin (RH1, 460–530 nm), rhodopsin-like (RH2, 450–535 nm), short-wavelength-sensitive 1 and 2 (SWS1, 355–440 nm; SWS2, 400–490 nm),

---

Corresponding Authors: sivakumar.sekharan@yale.edu; elsa.yan@yale.edu; victor.batista@yale.edu.

Supporting Information

Primary sequence alignment between SHUV and rhodopsin; complete refs 18,32,36; experimental and computational details. This information is available free of charge via the Internet at http://pubs.acs.org

Notes

The authors declare no competing financial interest.

and medium-/long-wavelength-sensitive (M/LWS, 490–570 nm).[1–6] In mammals, UV and violet SWS1 cone pigments are the immediate predecessors of rhodopsin (Figure 1A), since modern day mammals no longer have functional SWS2 pigments. Rhodopsin absorbs in the visible region and contains a protonated Schiff base of 11-*cis*-retinal (PSB11), whereas UV pigments contain an unprotonated Schiff base (USB11) linked to a conserved lysine residue. The structural factors that determine this distinct protonation state of the chromophore in UV pigments remain to be understood at the molecular level. Here, we address these fundamental structure/function relations in the Siberian hamster (*Phodopus sungorus*) UV (SHUV) cone photoreceptor.

The SHUV pigment gene (GenBank ID: JQ036217) was reverse transcribed from Siberian hamster retinal RNA (see Supporting Information, SI). The wild-type (WT), F86Y, S90A, and S90C SHUV genes (bovine rhodopsin numbering is used) were cloned into a tetracycline inducible pACMV-TetO vector after adding the 1D4 tag (the last nine amino acids of bovine rhodopsin C-terminus, TETSQVAPA) to the genes' C-termini.[7,8] The WT and SHUV mutants were expressed in GnTI-HEK293S stable cell lines[9] and prepared under dim red light. Using established procedures[10,11] the pigments were regenerated with 11-*cis* retinal and purified via immunoaffinity chromatography in 0.02% *n*-dodecyl β-D-maltoside. The dark-state spectrum of WT SHUV revealed that this pigment has an absorption maximum (λ_{max}) at 359 nm (Figure 2), consistent with the USB11 form.[12,13] Characterization of mutants reveals that S90A and S90C have almost identical spectra (λ_{max} of 358 nm), whereas the F86Y mutant has a more prominent UV band (376 ± 2 nm) at pH 6.6 and a more prominent visible band (432 ± 3 nm) at pH 5.1 (Figure 2). An acid denaturation assay showed that the absorption in the UV region is due to the dark-state species and not from free retinal resulting from protein instability (see Figure S2).

A comparative analysis of the spectroscopic properties of the SHUV WT and mutants clearly suggest that the interactions responsible for regulating the protonation state of the retinyl chromophore are preserved in S90A and S90C mutants, but significantly altered in the F86Y mutant. However, the nature of key electrostatic interactions and hydrogen-bonding networks (HBNs) responsible for steering the mechanism of spectral tuning remain largely unexplored. Here, we analyze the SHUV ligand environment as described by structural models of WT and mutant SHUV pigments. The models are based on the X-ray structure of bovine rhodopsin (PDB code: 1U19)[14] (Figure 1B) and are built by using density functional theory quantum mechanics/molecular mechanics (DFT QM/MM)[15] hybrid methods. The DFT QM/MM models were optimized according to the ONIOM hybrid method[16] with electronic-embedding (EE) scheme,[17] as implemented in Gaussian09[18] and as described in our previous studies on rhodopsin.[19,20] Models for WT, S90A, and S90C with USB linkages are compared to models of the F86Y mutant with both USB and PSB linkages that account for the two distinct spectral features in the UV (~376 nm) and visible (~432 nm) regions (Figure 2).

Although other pigments have higher homology with the SHUV (e.g., the human blue pigment with ~85% homology),[21] rhodopsin remains the most homologous pigment with a resolved X-ray crystal structure,[14] including internal water molecules that are thought to be essential for functionality of visual pigments.[22,23] The DFT QM/MM model of the SHUV

pigment contains 26 water molecules that are also conserved in rhodopsin (Figure 1B). Within 3.0 Å of the USB, there are 10 nonconserved residues present, including F86(M) and S90(G), with rhodopsin residues indicated in parentheses.[14] There are also eight conserved key active site residues, including E113, E181, S186, C187, Y268, and Y192 that participate in forming an extended HBN around the USB11 (see SI). T94 was also proposed to be part of this extended HBN in rhodopsin,[24] however, it is substituted by V94 in SHUV, a hydrophobic residue that disrupts the H-bonding connectivity in the active site.

In the DFT-QM/MM model of rhodopsin, an extended HBN is formed between Y268, E181, w2a, S186, C187, E113, and w2b (Figure 3, left).[19,20] The protonated form of the chromophore is stabilized by H-bonding with the negatively charged counterion E113 stabilized by w2b. However, with the USB11 in the SHUV pigment, the neutral (protonated) form of E113 is stabilized as a H-bond donor to S186, which in turn becomes a hydrogen-bond (HB) donor to E181 (Figure 3, right). Internal water molecules are essential for the stability of HBNs in the active site,[22,23] including w2c near sites F86 and G117. Since the USB11 is shown to be stabilized by the protonated form of E113, which is also H-bonded to S90, we suggest that the presence of w2b near the SB is neither likely nor necessary to occur in the SHUV pigment (see SI).

The UV–vis spectrum of the F86Y mutant exhibit two distinct peaks (~376 and ~432 nm), suggesting the coexistence of USB and PSB chromophores at equilibrium. The visible band was previously observed at 424 nm upon F86Y mutation in the mouse UV pigment and was attributed to the presence of a PSB in the pigment.[21] In fact, isolation of the two species was reported to be difficult in the F86Y/E113Q double mutant due to pH-dependent equilibrium,[21] also observed for the SHUV pigment although to a lesser extent. However, the molecular events underlying the transformation of USB11 to PSB11 upon F86Y mutation remained unexplored. We find that the F86Y mutation stabilizes H-bonds that establish an “interhelical lock” (IHL) between helices TM6, TM2, and TM3, with F86Y on TM2 functioning as a HB acceptor of Y265 in TM6, and as a HB donor to an internal water molecule (wat2c) that is H-bonded to the backbone of G117 on TM3 (Figure 4). The IHL is aided by HBNs between the side chain and the backbone groups of amino acid residues Y265, F86Y, w2c, S118, E113, and S90 and nonpolar residues G117 and A114, effectively establishing a strong contact between TM6, TM2, and TM3. Although Y268 is part of TM6, it is an HB acceptor to E181 in the EII loop and, therefore, is not as involved as Y265 in constraining the displacement of TM6. Displacement of the TM6 away from TM3 has been proposed to be a conformational change essential for the activation of rhodopsin and other GPCRs.[25–28] Comparison of the ONIOM QM/MM extrapolated energies reveals that F86Y mutant model with a PSB is more stable than with a USB by ~10 kcal/mol due to the presence of an IHL involving TM6, TM3 and TM2 helices (see section III of the SI).

Site 90 next to the USB in the SHUV pigment, involves the polar residue serine, which replaces the nonpolar residue glycine at the equivalent site in rhodopsin. The side chain of S90 forms a weak HB with E113, establishing an interaction that is not possible in rhodopsin. This additional HB, however, displaces an internal water molecule (w2b in rhodopsin) to the position of w2c in SHUV (Figure 3). To test the strength of key H-bonds responsible for the IHL of the SHUV pigment, we have analyzed models of the S90A and

S90C mutants. Upon S90A mutation, the HB between S90 and E113 as well as the interhelical contact between TM2 and TM3 are lost, which induces an increase in distance between the USB and E113 compared to the WT (from 3.41 to 3.54 Å, Figure 5). In contrast, the S90C mutant induces smaller changes, with only slight stretching of the HB between S90 and E113 (from 1.87 to 1.89 Å). The stretching reflects weakening of the HB since the -SH group of cysteine is a poor donor, compared to the -OH group of serine. This increase in distance between the USB and E113 upon mutation of S90 is consistent with the unprotonated form of the SB in mammalian UV pigments.

The weaker H-bonding interactions, induced by C90 could lead to destabilization of the interhelical contact between TM2 and TM3. Therefore, alterations in the HBN due to mutation of nonconserved residues at sites 86 and 90 may either prevent or promote the presence of a PSB in the active site. This is consistent with studies of avian SWS1 pigments (λ_{max} = 390–440 nm) where a shift of the absorption λ_{max}, from violet to UV, is induced by the F86S and S90C mutations.[5,6,29] The F86S mutation is characteristic to avian violet pigments, and an additional S90C mutation was assumed to cause deprotonation of the SB. It is thus plausible that the F86S mutation might induce formation of an IHL through HBNs as seen in the case of SHUV's F86Y mutant.

To validate the QM/MM structural models through direct comparisons to experimental data, we have computed the absorption spectra of the QM/MM models by using *ab initio* multireference methods, including the spectroscopy oriented configuration interaction (SORCI+Q) method[30] with 6-31G(d) basis set and Amber96 level of theory,[31] as implemented in the ORCA 2.6.19 program.[32] This methodology typically yields results in good agreement with experiments (within ±20 nm), as shown in our previous studies on related retinal proteins.[33]

The comparison of calculated and experimental data reported in Table 1 shows very good agreement between the experimental absorption band and the calculated electronic vertical excitations, predicting that the WT model absorbs at 369 nm due to the presence of the USB and protonated E113 at the active site. Compared to the WT, both S90A and S90C pigments exhibit a blue shift of ~6 nm as S90A absorbs at 363 nm and S90C absorbs at 364 nm, respectively. The small blue shift can be attributed to the loss of or weakening of the HB[34] between sites 90 and 113, due to the S90A and S90C mutations. In the case of the F86Y mutant, the QM/MM model with an USB absorbs at 382 nm, while the model with a PSB absorbs at 421 nm. The calculated values are in excellent agreement with the experimental measurements of ~376 and ~432 nm, respectively. Compared to the WT, the molecular origin of the spectral shifts can be traced back to the breaking (S90A) or weakening (S90C) of an intermolecular HB between S90 and E113 residues and to the formation of an HB involving the F86Y mutant (see Figure S5).

Another interesting finding revealed by our calculations is the excited state (S_1/S_2) level order reversal that correlates with the protonation state of the Schiff-base linkage (USB vs PSB) and corresponding protonation state of the counterion at the chromophore binding site.[35] Also, the change in magnitude of the dipole moment ($\Delta\mu$) between the ground and the excited states and increase or decrease in the oscillator (f) and rotatory (R) strengths offers

insight into the unique photophysical properties of the SHUV pigment. In this case, the dramatic decrease in f (from 1.62 to 0.35 au) and R (from 0.13 to 0.00 au) values due to S90A mutation confirms the loss of a HB between S90 and E113 essential for stabilization of the counterion position. Similarly, the significant increase in f (from 1.23 to 1.52 au) and $\Delta\mu$ (from 10.00 to 11.67 D) values upon F86Y mutation correlates well with the increase in the number of dipolar side chain groups in the active site that can enhance the dipole–protein charge interaction leading to a red (opsin) shift.[36]

In summary, we find that structural models of the WT and mutant SHUV pigments, validated through the analysis of their spectral properties and direct comparisons with experimental measurements, provide fundamental insights into the molecular origin of spectral tuning in ancestral photoreceptors. It is shown that formation of an IHL with specific amino acids, mediated by HBNs and internal water molecules, determines an arrangement of H-bonds at the active site that stabilize the unprotonated form of the Schiff-base linkage and, therefore, the unique photophysical properties of the SHUV pigment. The structural factors governing the protonation state of the chromophore and the spectral tuning mechanism involve not only amino acid residues in direct contact with the ligand but also an extended network of H-bonds establishing an IHL mechanism.

Supplementary Material

Refer to Web version on PubMed Central for supplementary material.

Acknowledgments

V.S.B acknowledges supercomputer time from NERSC and support from the National Science Foundation (NSF) grant CHE-0911520. E.C.Y.Y. acknowledges funding. Additional support was provided by a NSF fellowship DGE-0644492 to V.L.M. and by a NSF career grant MCB-0955407 to E.C.Y.Y.

References

1. Yokoyama S. Annu Rev Genomics Hum Genet. 2008; 9:259. [PubMed: 18544031]
2. Bowmaker JK. Vis Res. 2008; 48:2022. [PubMed: 18590925]
3. Shichida Y, Matsuyama T. Philos Trans R Soc B. 2009; 364:2881.
4. Hunt DM, Carvalho LS, Cowing JA, Davies WL. Philos Trans R Soc B. 2009; 364:2941.
5. Shi Y, Radlwimmer B, Yokoyama S. Proc Acad Natl Sci USA. 2001; 98:11731.
6. Shi Y, Yokoyama S. Proc Acad Natl Sci USA. 2003; 100:8308.
7. Chang BSW, Kazmi MA, Sakmar TP. Methods Enzymol. 2002; 343:274. [PubMed: 11665573]
8. Reeves PJ, Kim JM, Khorana HG. Proc Acad Natl Sci USA. 2002; 99:13413.
9. Reeves PJ, Callewaert N, Contreras R, Khorana HG. Proc Acad Natl Sci USA. 2002; 99:13419.
10. Oprian DD, Molday RS, Kaufman RJ, Khorana HG. Proc Acad Natl Sci USA. 1987; 84:8874.
11. Chan T, Lee M, Sakmar TP. J Biol Chem. 1992; 267:9478. [PubMed: 1577792]
12. Vought BW, Dukkipatti A, Max M, Knox BE, Birge RR. Biochemistry. 1999; 38:11287. [PubMed: 10471278]
13. Mooney VL, Szundi I, Lewis JW, Yan ECY, Kliger DS. Biochemistry. 2012; 51:2630. [PubMed: 22394396]
14. Okada T, Sugihara M, Bondar AN, Elstner M, Entel P, Buss VJ. Mol Biol. 2004; 342:571.
15. Warshel A, Levitt MJ. Mol Biol. 1976; 103:227.
16. Vreven T, Morokuma K, Farkas O, Schlegel HB, Frisch MJJ. Comput Chem. 2003; 24:760.

17. Bakowies D, Thiel W. J Phys Chem. 1996(100):10580.
18. Frisch, MJ., et al. Gaussian 09. Gaussian, Inc; Wallingford, CT: 2009. revision A.02
19. Gascón JA, Batista VS. Biophys J. 2004; 87:2931. [PubMed: 15339806]
20. Gascón JA, Sproviero EM, Batista VS. J Chem Theory Comput. 2005; 1:674.
21. Fasick JL, Applebury ML, Oprian DD. Biochemistry. 2002; 41:6860. [PubMed: 12022891]
22. Okada T, Fujiyoshi Y, Silow M, Navarro J, Landau EM, Shichida Y. Proc Natl Acad Sci USA. 2002; 99:5982. [PubMed: 11972040]
23. Katayama K, Furutani Y, Imai H, Kandori K. Angew Chem, Int Ed. 2010; 49:891.
24. Sugihara M, Buss V, Entel P, Hafner J. J Phys Chem B. 2004; 108:3673.
25. Farrens DL, Altenbach C, Yang K, Hubbell WL, Khorana HG. Science. 1996; 274:768. [PubMed: 8864113]
26. Sheikh SP, Zvyaga TA, Lichtarge O, Sakmar TP, Bourne HR. Nature. 1996; 383:347. [PubMed: 8848049]
27. Hubbell WL, Altenbach C, Hubbell CM, Khorana HG. Adv Protein Chem. 2003; 63:243. [PubMed: 12629973]
28. Altenbach C, Kusnetzow AK, Ernst OP, Hofmann KP, Hubbell WL. Proc Natl Acad Sci USA. 2008; 105:7439. [PubMed: 18490656]
29. Bowmaker JK, Heath LA, Wilkie SE, Hunt DM. Vis Res. 1997; 37:2183. [PubMed: 9578901]
30. Neese FA. J Chem Phys. 2003; 119:9428.
31. Cornell WD, et al. J Am Chem Soc. 1995; 117:5179.
32. Neese, F. ORCA. Vol. 2.6. Max Planck Institute; Muelheim an der Ruhr, Germany: 2007.
33. (a) Sekharan S, Altun A, Morokuma K. J Am Chem Soc. 2010; 132:15856. [PubMed: 20964383] (b) Sekharan S, Morokuma K. J Am Chem Soc. 2011; 133:4734. [PubMed: 21391708] (c) Sekharan S, Morokuma K. J Am Chem Soc. 2011; 133:19052. [PubMed: 22026715] (d) Sekharan S, Katayama K, Kandori H, Morokuma K. J Am Chem Soc. 2012; 134:10706. [PubMed: 22663599] (e) Sekharan S, Wei JN, Batista VS. J Am Chem Soc. 2012; 134:19536. [PubMed: 23145979] (f) Pal R, Sekharan S, Batista VS. J Am Chem Soc. 2013; 135:9624. [PubMed: 23777372]
34. Zhao GJ, Han KL. Acc Chem Res. 2012; 45:404. [PubMed: 22070387]
35. Birge RR, et al. Proc Natl Acad Sci USA. 1985; 82:4117. [PubMed: 2987964]
36. Mathies R, Stryer L. Proc Natl Acad Sci USA. 1976; 73:2169. [PubMed: 1065867]

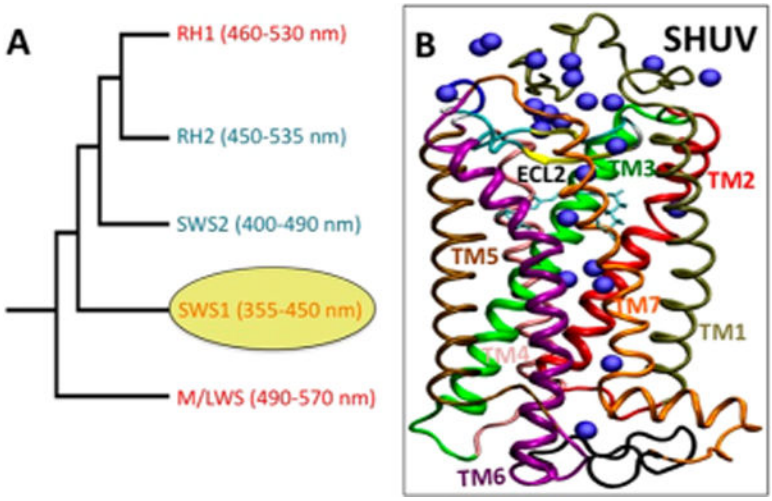

Figure 1.

(A) Cladogram depicting the evolution of the five classes of vertebrate visual pigments. Classes shown in blue are no longer expressed in nonmonotreme mammals. The SHUV pigment is classified under the SWS1 category highlighted in yellow. (B) DFT-QM/MM structural model of the WT SHUV pigment, with water molecules (blue spheres) and seven transmembrane helices TM1–TM7 (labeled cartoon) built as a homology model using the X-ray structure of bovine rhodopsin (PDB code: 1U19) as template.

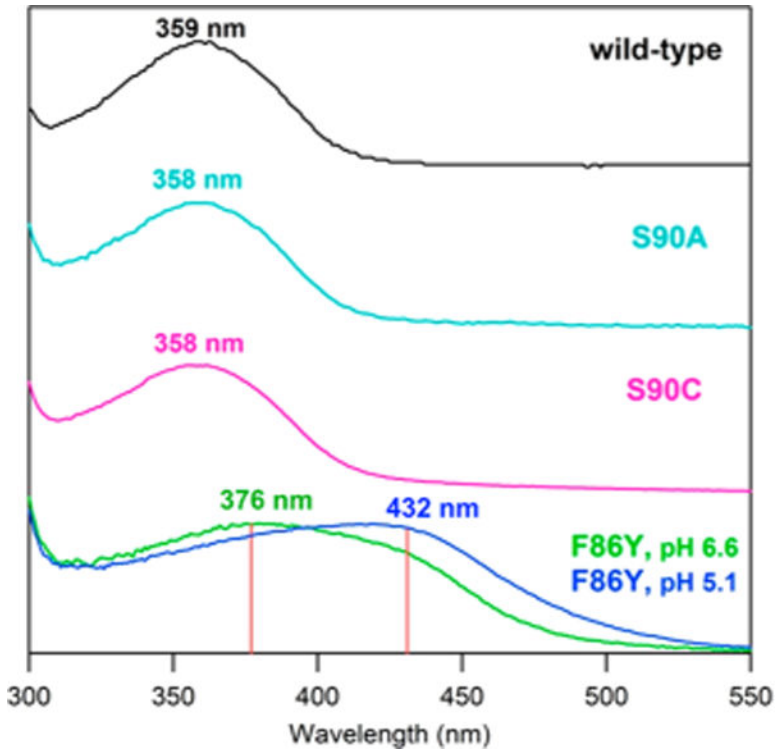

Figure 2.

UV–vis spectra of the WT, S90A, S90C, and F86Y mutant SHUV pigments. The F86Y mutant exhibits two distinct peaks. In the case of F86Y mutant, the relative population of USB and PSB is deeply dependent on the pH as indicated. We used IgorPro's multipeak fitting function to deconvolute the F86Y spectrum into two Gaussian peaks with λ_{max} (red lines) centered in the UV (376 ± 2 nm) and visible (432 ± 3 nm) regions.

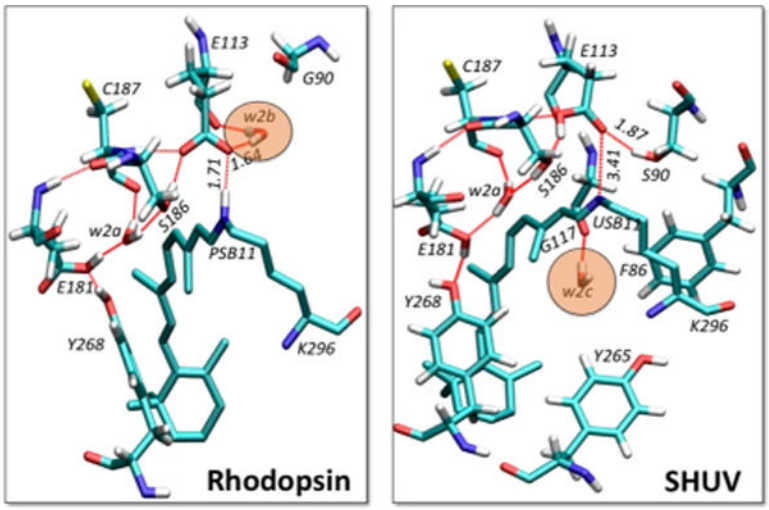

Figure 3.

Comparison of the DFT-QM/MM optimized WT rhodopsin (left) and SHUV (right) pigments. Water molecules, w2b and w2c are highlighted by shaded orange circles. Amino acid numbers correspond to the rhodopsin primary sequence. Distances between the Schiff-base NH and E113 in rhodopsin and SHUV are indicated, in addition to the H-bonding between w2b and E113 in rhodopsin and between S90 and E113 in SHUV.

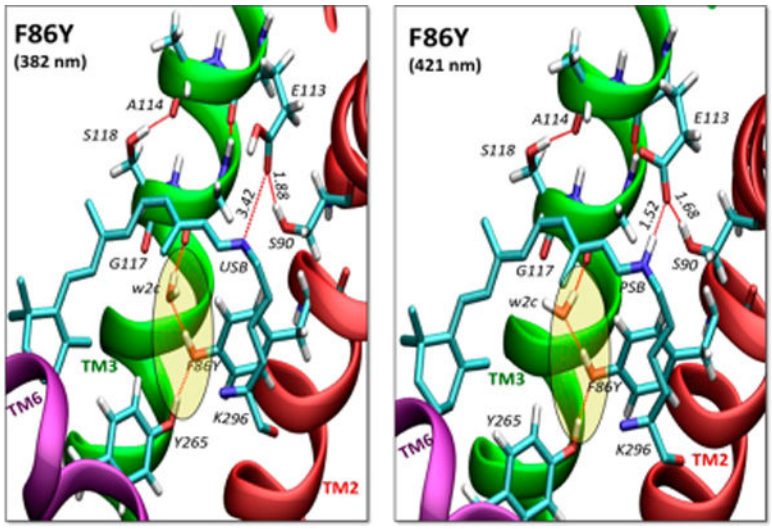

Figure 4.

DFT QM/MM models of the F86Y mutant with USB (left) and PSB (right) linkages, revealing an IHL (shaded region) between TM6 (purple), TM3 (green), and TM2 (red) by H-bonding (red dashed lines) of w2c and polar side chains or backbone groups of amino acid residues Y265, F86Y, G117, S118, A114, E113, and S90.

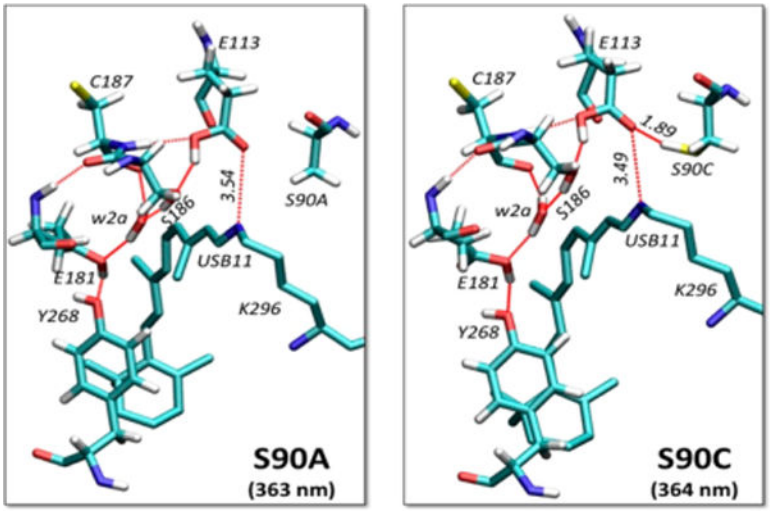

Figure 5.

Comparison of the QM/MM optimized models of S90A (left) and S90C (right) SHUV mutants. HBNs comprised of S90, E113, S186, S187, w2a, E181, and Y268 residues are shown in red dashed lines. Distances between USB and E113 and between S90C and E113 are indicated in Å.

Table 1

Comparison of Calculated and Experimental Absorption Bands, Including the Wavelength of Maximum Absorption (λ) in nm, Oscillator (f) and Rotatory (R) Strengths in au, and the Change in the Ground- (S_0) and Excited-State (S_2 for USB; S_1 for PSB) Dipole Moments ($\Delta\mu$) of USB11 and/or PSB11 in the Protein (QM/MM) Environments of WT, F86Y, S90A, and S90C SHUV Pigment Models[a]

	first vertical excited-state properties				
	protein				
SHUV pigment models	λ	f	R	$\Delta\mu$	**expt.**
$^{\text{strong HB}}$WT/USB11	369 (0)	1.62	0.13	11.26	359 (0)
F86Y/USB11$^{+10.392}$	382 (+13)	1.23	0.10	10.00	376 (+17)
F86Y/PSB11$^{0.000}$	421 (+39)	1.52	0.04	11.67	432 (+56)
$^{\text{broken HB}}$S90A/USB11	363 (−6)	0.35	0.00	5.18	358 (−1)
$^{\text{weak HB}}$S90C/USB11	364 (−5)	1.60	0.09	11.13	358 (−1)

[a] Strong, weak, and broken HB refers to the nature of the HB between S90 and E113. Numbers in superscript refer to the relative energies, whereas numbers in parentheses indicate the spectral shift relevant to the WT/USB11 model, except for F86Y/PSB11, which is referenced against F86Y/USB11.